Glutamic Acid Dendrimers Attached to a Central Ferrocene Core: Synthesis and Properties

Francis E. Appoh, Donald S. Thomas, and Heinz-Bernhard Kraatz*

Department of Chemistry, University of Saskatchewan, 110 Science Place, Saskatoon, Saskatchewan S7N 5C9, Canada

Received March 11, 2005; Revised Manuscript Received July 11, 2005

ABSTRACT: The first synthesis of a series of glutamic acid based dendrimers having a central ferrocene core is described. The materials were fully characterized spectroscopically and display strong intramolecular H-bonding. This H-bonding can be disrupted with DMSO. The redox properties of the core are attenuated by the increase in the peptide dendritic sphere. But even at generation 6, there is communication between the exterior and the redox core.

Introduction

Electron delocalization in dendrimeric systems may have potential applications in electroluminescent devices, thin-film transistors, NLO materials, and artificial photosynthesis systems.[1−4] There are several examples in which redox-active groups have been incorporated into the interior of dendritic molecules. It was shown that the dendritic architecture modulates the physical properties of the core.[5−8] In electrochemical experiments, the dendritic sheath in general presents sufficient steric hindrance to a redox-active core to approach the electrode, resulting in slow kinetics.[6,7,9−11] Importantly, a change in the dendrimer size can lead to changes in the thermodynamic properties of the redox probe as measured by its redox potential. For example, the ferrocene core in benzyl ether dendrimers having the dendrimer attached only on one side of the bipy core does not show any change in the redox potential with increasing dendritic generation.[64,65] However, the redox potential of the same core placed into a symmetric ferroceneimine-based dendrimer strongly increase with increasing dendrimer size.[5−7,9] In addition, its redox potential is strongly solvent dependent.[11] Dendrimers having a ferrocene core were investigated by Kaifer and co-workers.[6,7,9,10] The redox potential exhibit interesting influences as a function of dendrimer size and exterior dendrimer surface. For example, dendrimer esters in dichloromethane solution exhibit a reduction of the Fc redox potential with increasing dendrimer generation, whereas the redox potential of the acid-terminated dendrimers increases with increasing generation in water.[6,7,9,10] A similar behavior was displayed by Fe−porphyrin dendrimers in which the redox potential of the Fe(II)/Fe(III) couple in dichloromethane is independent of dendrimer generation, but in aqueous media it greatly reduced with increasing generations, which was assigned to an enhanced solvation of the Fe−porphyrin in the lower dendrimer generations.[8] Gorman and coworkers have hypothesized that primary structural elements that enforce backfolding should increase the degree of steric congestion around the core moiety of the dendrimer, and for redox cores, this should have a profound effect on its properties.

* Corresponding author: Fax +1-306-966-4730; Tel +1-306-966-4660; e-mail kraatz@skyway.usask.ca.

Our general interest in the properties of ferrocene (Fc)−peptide conjugates[12−18] led us to explore the generational effect in peptide dendrimers on the redox properties of a central Fc group. Although there are several examples of peptide-based dendrimers,[19−25] including L-glutamic acid-based dendrimers,[26−32] the synthesis of Fc-based peptide dendrimers has not been reported in the literature to date.

Our work described here is aimed at investigating the effect of peptide dendrimer generation on the electroactive Fc core. Does encapsulation result in complete shielding of the electroactive core? This question is in particular important in light of the recent investigations into the electron transfer through peptides, which appear to suggest that electron transfer is efficient in peptides in some cases. Here, we report the synthesis, characterization, and properties of the first bioorganometallic peptide dendrimers from generation 1 (**G1**) to generation 6 (**G6**) having a glutamic acid-based dendrimers connected to a monosubstituted central Fc core.

Experimental Section

General Methods. All syntheses were carried out in air unless otherwise indicated. CH_2Cl_2 and $CHCl_3$ (BDH, ACS grade) used for synthesis, FT-IR, and electrochemistry were dried (CaH_2) and distilled under N_2 prior to use. Acetone, EtOAc, CH_3CN, MeOH, diethyl ether (BDH, ACS grade), hexanes (Fischer, HPLC grade), $CHCl_3$, and CH_2Cl_2 (HPLC grades) used for the purpose of purification were used as received. $CDCl_3$ and CD_3CN (Aldrich) were dried by and stored over molecular sieves (8−12 mesh, 4 Å effective pore size; Fisher) before use. Acetone-d_6 (MSD) was used as received. EDC, HOBt, H-Glu-OEt·HCl (Aldrich), HBTU (SynPep), Boc-GluOH (Aldrich), $MgSO_4$, and $NaHCO_3$ (VWR) were used as received. Et_3N (BDH, ACS grade) used in Fc−amino acid couplings was dried by molecular sieves when used in stoichiometric quantities. For column chromatography, a column with a width of 2.7 cm (i.d.) and a length of 45 cm was packed 18−22 cm high with 230−400 mesh silica gel (VWR). For TLC, aluminum plates coated with silica gel 60 F254 (EM Science) were used. NMR spectra were recorded on a Bruker AMX-500 spectrometer operating at 500 MHz (1H) and 125 MHz ($^{13}C\{1H\}$). Peak positions in both ^1H and ^{13}C spectra are reported in ppm relative to TMS. ^1H spectra of all other compounds are referenced to the residual $CHCl_3$ signal at δ 7.25. All $^{13}C\{1H\}$ spectra are referenced to the $CDCl_3$ signal at δ 77.23. Analytical HPLC was performed on a Varian ProStar system equipped with a C18 reverse phase column with a flow rate of 0.5 mL min^{-1}. Monitoring was done at

10.1021/ma050531d CCC: $30.25
Published on Web 08/13/2005

wavelength of 215 nm eluting with 2−98% MeCN/0.1% TFA over 200 min. Circular dichroism (CD) measurements were carried out on a π^* 180 spectrometer, using hplc grade solvents and quartz glass cuvettes with a 1 mm path length. Mean residue molar ellipticities were calculated according to the following equation

$$[\theta] = \frac{[\theta]_{obs}}{10lcn}$$

where $[\theta]_{obs}$ is the observed ellipticity measured in degrees, l is the path length of the cell in centimetres, c is molar concentration of the peptide, and n is the number of amino acid residues.

Synthesis of G1. To a stirring mixture of Fc-COOH (1.0 g, 4.3 mmol) and HOBt (0.79 g, 5.2 mmol) in CH_2Cl_2 (40 mL) at room temperature, solid EDC (0.99 g, 5.2 mmol) is added, causing the orange slurry to slowly change into a clear solution. In a separate flask, H-Glu-OEt·HCl (1.1 g, 4.73 mmol) is dissolved in CH_2Cl_2 (10 mL), and Et_3N (0.5 mL, 6.6 mmol) and is then added to the stirring reaction mixture. After stirring overnight, the reaction solution is washed consecutively with aqueous solutions of saturated $NaHCO_3$, 10% citric acid, saturated $NaHCO_3$, and finally with distilled water. The organic phase is dried by anhydrous Na_2SO_4 and filtered, and the solvent is removed under reduced pressure, giving the crude orange product. The product is purified by column chromatography (R_f = 0.3; hexane/EtOAc/$CHCl_3$ 1:1:2), giving an orange solid. Yield: 90%, 1.45 g. Calcd for $C_{20}H_{25}NO_5Fe$: 415.1082 $[M + 1]^+$; found: 415.1401. FT-IR (cm^{-1}, KBr): 3455, 3344 (w, br), 1746 (s, C=O ester), 1640 (s, amide I), 1547 (s, amide II). UV−vis ($CHCl_3$, λ_{max} in nm, ϵ in cm^{-1} M^{-1}): 442 (422). ^1H NMR (δ in ppm $CDCl_3$): 6.55 (1H, d, J = 7.4 Hz NH), 4.20 (1H, m, H^{α}−Glu), 3.90 (2H, q, J = 7.1 Hz, OCH_2), 4.09 (4H, q, J = 7.1 Hz, OCH_2), 4.75 (1H, s, H^o), 4.66 (1H, s, H^o), 4.35 (2H, s, CH^m Cp), 4.25 (5H, s, Cp), 1.20 (3H, t, J = 7.1 Hz, CH_3), 1.16 (3H, t, J = 7.1 Hz, CH_3). $^{13}C\{^1H\}$ NMR (δ in ppm, $CDCl_3$): 173.6, 172.4, 170.3 (C=O), 75.6 (C^i), 70.9 (C), 70.1 (unsubst Cp), 68.5 (Cm), 52.1 (CH^{α}−Glu), 27.2 (CH_2−Glu), 30.8 (CH_2−Glu), 61.7, 61.0 (CH_2−O), 14.4 (CH_3).

Synthesis of Boc-G2. To a stirring mixture of compound Boc-GluOH (1.80 g, 7.4 mmol) and HOBt (2.50 g, 16 mmol) in CH_2Cl_2 (50 mL) at room temperature, solid EDC (3.10 g, 16.0 mmol) was added. In a separate flask, H-Glu-OEt·HCl (4.50 g, 18.0 mmol) was dissolved in CH_2Cl_2 (10 mL), and Et_3N (1.2 mL, 16.0 mmol) and is then added to the stirring reaction mixture. After stirring 36 h, the reaction was worked up as described above. The organic phase was dried over anhydrous Na_2SO_4 and filtered, and the solvent was removed under reduced pressure. The crude product was purified by column chromatography (R_f = 0.4; 10%MeOH/$CHCl_3$). Yield: 73%, 3.70 g. ^1H NMR ($CDCl_3$, δ in ppm): 7.88 (1H, d, J = 8.6 Hz, NH), 7.65 (1H, d, J = 8.3 Hz, NH), 5.02 (1H, d, J = 7.2 Hz, NH), 4.72 (1H, m, H^{α}−Glu), 4.65 (1H, m, H^{α}−Glu), 3.96 (1H, m, H^{α}−Glu), 2.45 (4H, m, CH_2 of Glu), 2.33 (6H, m, CH_2 of Glu), 1.87 (4H, m, CH_2 of Glu), 4.13 (8H, m, OCH_2), 1.12 (3H, t, CH_3),1.42 (9H, s, CH_3 of Boc). $^{13}C\{^1H\}$ NMR (δ in ppm, $CDCl_3$): 173.0, 172.9, 172.8, 172.6, 172.3 (C=O),156.1 (C=O Boc), 79.2, (C−O Boc), 55.7, 55.6, 53.9 (CH_2−O ester), 61.3, 60.7 (C^{α} of Glu), 32.4, 30.5, 26.0, 26.0, (CH_2 Glu), 25.9, 13.2 (CH_3).

Synthesis of G2. To a stirring mixture of FcCOOH (0.36 g, 1.5 mmol) and HOBt (0.23 g, 1.69 mmol) in CH_2Cl_2 (50 mL) at room temperature, solid EDC (0.29 g, 1.69 mmol) is added, causing the orange slurry to slowly change into a clear solution. In a separate flask containing **Boc-G2** (1.09 g, 6.6 mmol) dissolved in CH_2Cl_2 (10 mL), the Boc group was deprotected with TFA, neutralized with Et_3N (0.5 mL, 6.6 mmol), and is then added to the stirring reaction mixture. After stirring overnight, the reaction solution is washed consecutively with saturated $NaHCO_3$, 10% citric acid, saturated $NaHCO_3$, and finally with distilled water. The organic phase is dried over anhydrous Na_2SO_4 and filtered, and the solvent is removed under reduced pressure, followed by column chromatography (R_f = 0.7; 5% MeOH/$CHCl_3$, R_f = 0.3 hexane/MeOH/$CHCl_3$ 4:1:15), giving an orange solid. Yield: 65%. 0.70 g. Calcd for $C_{34}H_{48}N_3O_{11}Fe$: 730. 2638 $[M + 1]^+$; found: 730.2630. FT-IR (cm^{-1}, KBr): 3455, 3302 (NH), 1746 (s, C=O ester), 1640 (s, amide I), 1547 (s, amide II). UV−vis ($CHCl_3$, λ_{max} in nm, ϵ in cm^{-1} M^{-1}): 440 (413). ^1H NMR ($CDCl_3$, δ in ppm): 8.10 (1H, d, J = 8.4 Hz, NH), 7.69 (1H, d, J = 8.6 Hz, NH), 6.40 (1H, d, J = 7.6 Hz, NH), 4.71 (1H, s, H^{α}−Cp), 4.66 (1H, s, H^{α}−Cp), 4.32 (2H, s, H_m−Cp), 4.19 (5H, s, Cp), 4.24 (4H, m, OCH_2), 4.14 (4H, m, OCH_2), 4.68 (1H, m, CH^{α}−Glu), 4.34 (1H, m, H^{α}−Glu), 2.48 (5H, m, CH^{α}−Glu), 2.29 (5H, m, CH^{α}−Glu), 2.28 (5H, m, CH^{α}−Glu), 1.29 (12H, m, CH_3). $^{13}C\{^1H\}$ NMR (δ in ppm, $CDCl_3$): 174.0, 173.9, 173.2, 173.0, 172.9, 172.6, 170.6 (C=O), 75.6 (C^i), 70.9 (C^o), 70.1 (Cp), 68.6 (C^m), 62.6, 62.5, 61.1, 61.0 (CH_2−O), 52.5, 52.2, 52.1 (C^{α} of Glu), 32.7, 31.1, 30.9, 29.5, 27.2, 27.1 (CH_2 of Glu), 14.6, 14.5 (CH_3).

Synthesis of Boc-G3. To a stirring mixture of compound Boc-GluOH (0.25 g, 1.0 mmol) and HOBt (0.34 g, 2.2 mmol) in CH_2Cl_2 (25 mL) at room temperature, solid EDC (0.42 g, 2.2 mmol) is added. In a separate flask, **Boc-G2** (1.70 g, 2.4 mmol) is deprotected with TFA in CH_2Cl_2 (20 mL) and neutralized with Et_3N (0.6 mL, 8.0 mmol) and then added to the reaction mixture. After stirring for 36 h, the reaction solution was subjected to the aqueous workup as described for the other systems (vide supra). After evaporation of the organic phase, the crude product is purified by column chromatography (R_f = 0.4; 10%MeOH/$CHCl_3$). Yield: 64%, 0.80 g. ^1H NMR ($CDCl_3$, δ in ppm): 8.55 (1H, d, J = 8.6 Hz, NH), 8.28 (2H, d, J = 8.3 Hz, NH), 7.79 (1H, d, J = 7.9 Hz, NH), 7.54 (1H, d, J = 7.6 Hz, NH), 4.95 (1H, d, J = 7.1 Hz, NH), 4.84 (1H, m, CH^{α}−Glu), 4.68 (1H, m, CH^{α}−Glu), 3.96 (1H, m, CH^{α}−Glu), 2.46 (14H, m, CH_2 of Glu), 2.27 (14H, m, CH_2 of Glu), 4.23 (8H, m, OCH_2), 4.13 (8H, m, OCH_2), 1.29 (24H, m, CH_3), 1.46 (9H, s, CH_3 of Boc). $^{13}C\{^1H\}$ NMR (δ in ppm, $CDCl_3$): 174.5, 174.4, 174.19, 173.0, 172.8, 172.7 (C=O), 155.4 (C=O of Boc), 62.7, 62.6, 62.5, 61.1, 60.9, 60.5 (OCH_2), 53.8, 53.5, 52.1, 51.9 (C^{α} of Glu), 32.5, 31.7, 31.2, 30.8, 30.5, (CH_2 of Glu), 27.7 (CH_3 of Boc), 14.6, (CH_3).

Synthesis of G3. To a stirring mixture of FcCOOH (0.15 g, 0.6 mmol) and HOBt (0.11 g, 0.68 mmol) in CH_2Cl_2 (25 mL) at room temperature, solid EDC (0.14 g, 0.68 mmol) was added, causing the orange slurry to slowly change into a clear solution. In a separate flask, TFA was added to a solution of **Boc-G3** in CH_2Cl_2 (10 mL). The solution was neutralized with Et_3N (0.5 mL, 6.6 mmol) and is then added to the stirring reaction mixture. After stirring overnight, the product was isolated as described above. The product was purified by column chromatography (R_f = 0.7; 5%MeOH/$CHCl_3$, R_f = 0.3 hexane/MeOH/$CHCl_3$ 4:1:15), giving an orange solid. Yield: 0.40 g, 50%. Calcd for $C_{62}H_{91}N_7O_{23}Fe$: 1358.5515 $[M + 1]^+$; found: 1358.5489. FT-IR (cm^{-1}, KBr): 3292 (s, br amide A), 1736 (s, C=O ester), 1642 (s, amide I), 1535 (s, amide II). UV−vis ($CHCl_3$, λ_{max} in nm, ϵ in cm^{-1} M^{-1}): 444 (394). ^1H NMR ($CHCl_3$, δ in ppm): 8.63 (1H, d, J = 6.68 Hz, NH), 8.23 (1H, d, J = 9.16 Hz, NH), 8.20 (1H, d, J = 7.1 Hz, NH), 8.14 (1H, d, J = 8.77 Hz, NH), 7.85 (1H, d, J = 9.0 Hz, NH), 7.72 (1H, d, J = 8.8 Hz, NH), 6.02 (1H, d, J = 8.0 Hz, NH), 4.61 (2H, s, H−Cp), 4.26 (2H, s, H^m−Cp), 4.14 (5H, s, H−Cp), 4.14 (2H, m, OCH_2), 4.85 (1H, m, H^{α}−Glu), 4.60 (1H, m, CH^{α}−Glu), 4.21 (1H, m, CH^{α}−Glu), 4.11 (2H, m, H^{α}−Glu), 2.43 (14H, m, CH_2 of Glu), 2.27 (14H, m, CH_2 of Glu), 1.24, 1.12 (24H, m, CH_3). $^{13}C\{^1H\}$ NMR (δ in ppm, $CHCl_3$): 174.6, 174.4, 174.3, 174.1, 174.0, 173.9, 173.6, 173.0, 172.9, 172.3, 169.7 (C=O), 75.9 (C^i), 70.7 (C^o), 70.1 (Cp), 68.5 (C^m), 62.7, 62.5, 61.0, 60.7 (OCH_2) 53.7, 53.4, 52.1, 52.0, 51.9, 51.5 (CH^{α}−Glu), 32.5, 31.9, 31.1, 30.8, 30.6, 30.2, 28.0, 27.8, 27.5, 26.9 (CH_2 Glu), 14.6, 14.5 (CH_3).

Synthesis of Boc-G4. To a stirring mixture of compound Boc-GluOH (2.50 g, 4.3 mmol) and HOBt (2.90 g, 19.0 mmol) in CH_2Cl_2 (200 mL) at room temperature, solid EDC (3.60 g, 19.0 mmol) was added. In a separate flask, **Boc-G3** (2.10 g, 9.0 mmol) was dissolved in CH_2Cl_2 (100 mL) and Et_3N (1.5 mL, 19.0 mmol) and then added to the stirring reaction mixture. After further stirring 48 h, the reaction was worked up as described above. Saturated NaCl was required to break up the emulsion formed during the workup stages. The crude

product was purified by column chromatography (R_f = 0.4; 10%MeOH/$CHCl_3$). Yield: 2.30 g 36%. ^{1}H NMR ($CDCl_3$, δ in ppm): 8.2−7.37 (10H, m, NH,), 7.01 (3H, m, NH), 5.7 (1H, m, NH), 5.41 (1H, m, NH), 4.76−4.48 (1H, m, CH^{α}−Glu), 2.45 (4H, m, CH_2 of Glu), 2.21 (6H, m, CH_2 of Glu), 1.96 (4H, m, CH_2 of Glu), 4.21−4.13 (8H, m, CH_2), 1.27 (48H, m, CH_3 of ester), 1.42 (9H, s, CH_3 of Boc). $^{13}C\{^1H\}$ NMR (δ in ppm, $CDCl_3$): 173.9, 173.0 (C=O), 156.2 (C=O Boc), 78.9 (C−O Boc), 62.6, 62.4, 61.1 (CH_2−O ester), 52.9, 52.2, 27.2 (C^{α} of Glu), 32.3, 31.0, 30.8, 30.1, 27.2 (CH_2−Glu), 14.5 (CH_3 ester).

Synthesis of G4. A solution of **Boc-G4** in CH_2Cl_2 (50 mL) was deprotected with TFA (2.0 g, 1.38 mmol), then neutralized (Et_3N, 0.5 mL, 6.6 mmol), and then added to a stirring solution of FcOBt (0.45 g, 0.6 mmol) in CH_2Cl_2 (100 mL) preprepared from FcCOOH/HOBt/EDC. After 24 h, the reaction mixture was worked up as described above. The crude product is purified by column chromatography (R_f = 0.7; 5% MeOH/$CHCl_3$ and then R_f = 0.3 hexane/MeOH/$CHCl_3$ 4:1:15), giving an orange solid. Yield: 0.80 g, 25%. Calcd for $C_{118}H_{179}N_{15}O_{47}$-Fe: 2615.1427, $[M + 1]^+$; found: 2615.1322. FT-IR (cm^{-1}, KBr): 3303 (w, br amide A), 1735 (s, C=O ester), 1647 (s, amide I), 1541 (s, amide II). UV−vis ($CHCl_3$, λ_{max} in nm, ϵ in cm^{-1} M^{-1}): 446 (292). ^{1}H NMR ($CDCl_3$, δ in ppm): 8.75 (1H, d, J = 6.3 Hz, NH), 8.69 (1H, d, J = 5.4 Hz, NH), 8.63 (2H, d, J = 9.5 Hz, NH), 8.17 (2H, m, NH), 8.09 (2H, m, NH), 8.00 (2H, m, NH), 7.89 (1H, d, J = 8.8 Hz, NH), 7.77 (2H, d, J = 7.3 Hz, NH), 7.69 (1H, d, J = 7.6 Hz, NH), 6.48 (1H, d, J = 7.6 Hz, NH), 4.59 (2H, s, H^{o}−Cp), 4.23 (2H, s, H^{m}−Cp), 4.10 (5H, s, Cp), 4.20−4.03 (2H, m, OCH_2), 4.75−3.58 (15H, m, H^{α}−Glu), 2.38, 2.13, 1.91 (64H, m, CH_2 of Glu), 1.24, 1.16 (48H, m, CH_3). $^{13}C\{^1H\}$ NMR (δ in ppm, $CHCl_3$): 175.6, 175.4, 174.7, 174.5, 174.3, 173.7, 173.5, 173.3, 173.0, 172.9, 172.8, 172.7, 172.5, 172.3, 172.2, 171.0, 169.8 (C=O), 77.0 (C^{i}), 70.7 (C^{o}), 70.1 (Cp), 68.4 (C^{m}), 62.6, 62.5, 61.1, 61.0, 60.9 (OCH_2) 53.7, 53.4, 52.1, 52.0, 51.9, 51.5, 49.6 (CH^{α}−Glu), 34.29, 32.4, 31.0, 30.8, 30.1, 29.7, 28.8, 28.7, 27.1, 27.0, 26.0, 25.9, 25.3 (CH_2−Glu), 14.5 (CH_3).

Synthesis of Boc-G5. To a stirring mixture of Boc-GluOH (0.25 mg, 1.0 mmol) and HOBt (0.34 mg, 2.2 mmol) in CH_2Cl_2 (25 mL) at room temperature, solid EDC (0.42 mg, 2.2 mmol) is added. In a separate flask, **Boc-G4** (1.70 g, 2.4 mmol) is deprotected with TFA in CH_2Cl_2 (20 mL) and neutralized with Et_3N (0.6 mL, 8.0 mmol) and then added to the reaction mixture. After stirring for 36 h, the reaction solution was subjected to the queous workup as described for the other systems (vide supra). After evaporation of the organic phase, the crude product is purified by column chromatography (R_f = 0.4; 10% MeOH/$CHCl_3$). Yield: 33%, 0.80 g. ^{1}H NMR ($CDCl_3$, δ in ppm): 8.18−7.28 (31H, NH), 4.84 (1H, m, CH^{α}−Glu), 4.80−4.58 (31H, m, CH^{α}−Glu), 2.47−1.8 (124H, m, CH_2 of Glu), 4.13−4.05 (64H, m, OCH_2), 1.21−1.17 (96H, m, CH_3), 1.42 (9H, s, CH_3 of Boc). $^{13}C\{^1H\}$ NMR (δ in ppm, $CDCl_3$): 174.2, 174.1, 173.9, 173.8, 173.4, 173.2, 172.7, 172.6, 172.5, 172.3 all (C=O), 156.3 (C=O of Boc), 78.6 (C−O Boc), 62.5, 62.2, 62.1, 60.5, 60.6, 60.4 (OCH_2) 53.4, 53.3, 53.0, 51.7, 51.6, 51.5, 51.4 (CH^{α}−Glu), 33.7, 32.0, 31.9, 30.7, 27.4, 27.2, 27.0, 26.8, 26.5, 26.2 (CH_2−Glu), 14.4, 14.8 (CH_3).

Synthesis of G5. To a stirring mixture of FcCOOH (0.15 g, 0.6 mmol) and HOBt (0.11 g, 0.68 mmol) in CH_2Cl_2 (25 mL) at room temperature, solid EDC (0.14 g, 0.68 mmol) was added, causing the orange slurry to slowly change into a clear solution. In a separate flask, TFA was added to a solution of **Boc-G5** in CH_2Cl_2 (10 mL). The solution was neutralized with Et_3N (0.5 mL, 6.6 mmol) and is then added to the stirring reaction mixture. After stirring overnight, product was isolated as described above. The product was purified by column chromatography (R_f = 0.7; 5%MeOH/$CHCl_3$). Yield: 0.40 g, 50%. Calcd for $C_{230}H_{355}N_{31}O_{63}Fe$: 4616.4876 $[M + 1]^+$. FT-IR (cm^{-1}, KBr): 3289 (s, br amide A), 1736 (s, C=O ester), 1657, 1643 (s, amide I), 1544, 1536 (s, amide II).

UV−vis ($CHCl_3$, λ_{max} in nm, ϵ in cm^{-1} M^{-1}): 432 (151). ^{1}H NMR ($CHCl_3$, δ in ppm): 8.18−7.26 (31H, NH), 4.13−4.04 (64H, m, OCH_2), 4.81−4.59, 3.61−3.21 (31H, m, H^{α}−Glu), 2.43−1.88 (124H, m, CH_2 of Glu), 1.22−1.17 (96H, m, CH_3), 1.42 (9H, m, Boc). $^{13}C\{^1H\}$ NMR (δ in ppm, $CHCl_3$): 173.8, 173.4, 172.4, 172.6, 172.2, 171.0, 170.0 (C=O), 69.7, 69.6, 68.0 (Cp), 62.2, 62.1, 60.7, 60.6, 60.3, 60.2 (OCH_2) 52.3, 52.0, 51.9, 51.7 (CH^{α}−Glu), 32.0, 31.7, 30.7, 30.5, 30.3, 30.2, 28.0, 26.8, 26.5 (CH_2−Glu), 14.0, (CH_3).

Synthesis of Boc-G6. To a stirring mixture of Boc-GluOH (0.04 g, 0.15 mmol) and HOBt (0.05 g, 0.15 mmol) in CH_2Cl_2 (100 mL) at room temperature, solid HBTU (0.12 g, 0.34 mmol) is added. In a separate flask, **Boc-G5** (1.3 g, 0.35 mmol) is deprotected with TFA in CH_2Cl_2 in CH_2Cl_2 (50 mL), neutralized with Et_3N (0.6 mL, 8.0 mmol), and then added to the reaction mixture. After stirring for 6 days, the reaction solution was subjected to the aqueous workup as described for the other systems (vide supra). After evaporation of the organic phase, the crude product is purified by column chromatography (R_f = 0.4; 10% MeOH/$CHCl_3$). Yield: 50%, 1.3 g. ^{1}H NMR ($CDCl_3$, δ in ppm): 8.64−7.27 (63H, NH), 4.16, 4.20, 4.30 (9H, Cp), 4.87, 4.85, 4.84, 4.69, 4.67, 4.66 (63H, m, CH^{α}−Glu), 2.52, −1.93 (256H, m, CH_2 of Glu), 4.22, 4.21, 4.20, 4.17, 4.16, 4.14, 4.12, 4.12, 4.10 (128H, m, OCH_2), 1.29, 1.28, 1.27, 1.26, 1.25, 1.23, 1.22 (192H, m, CH_3), 1.32 (9H, s, CH_3 of Boc). $^{13}C\{^1H\}$ NMR (δ in ppm, $CDCl_3$): 174.3, 174.1, 174.0, 173.9, 173.8, 173.4, 173.0, 172.7, 172.6, 172.5, 172.4, 172.3, (C=O), 156.1 (C=O Boc), 78.8 (C−O Boc), 62.3, 62.2, 62.0, 60.5, 60.6, 60.4 (OCH_2) 53.4, 53.3, 53.0, 51.7, 51.6, 51.5, 51.4 (CH^{α}−Glu), 33.2, 32.0, 31.9, 30.7, 30.2, 30.0, 27.4, 27.3, 27.2, 27.0, 26.8, 26.5, 26.4 (CH_2−Glu), 14.2, 14.1, 14.0 (CH_3).

Synthesis of G6. To a stirring mixture of FcCOOH (0.07 g, 0.3 mmol) and HOBt (0.04 g, 0.30 mmol) in CH_2Cl_2 (100 mL) at room temperature, solid HBTU (0.11 g, 0.30 mmol) was added. In a separate flask, TFA was added to a solution of **Boc-G6** (1.1 g, 0.34 mM) in CH_2Cl_2 (200 mL). The solution was neutralized with Et_3N (0.5 mL, 6.6 mmol) and is then added to the stirring reaction mixture. After stirring 3 days, product was isolated as described above. The product was purified by column chromatography (R_f = 0.7; 5% MeOH/$CHCl_3$), giving a light yellow solid. Yield: 0.6 g, 40%. Calcd for $C_{454}H_{707}N_{63}O_{127}Fe$: 7659.2419 $[M + 1]^+$. FT-IR (cm^{-1}, KBr): 3291, (s, br amide A), 1737 (s, C=O ester), 1657, 1641 (s, amide I), 1546, 1535 (s, amide II). UV−vis ($CHCl_3$, λ_{max} in nm, ϵ in cm^{-1} M^{-1}): 427 (64). ^{1}H NMR ($CHCl_3$, δ in ppm): 8.98−7.68 (63H, NH), (H Cp could not be distinguished), 4.14 (2H, m, OCH_2), 4.86, 4.66, 4.65 (63H, m, CH^{α}−Glu), 4.22, 4.21, 4.18, 4.16, 4.14, 4.12, 4.10 (128H,m, OCH_2), 2.44, 2.42, 2.40, 2.23, 2.23, 2.22, 2.20, 1.94, 1.93 (252H, m, CH_2 of Glu), 1.24, 1.14, 1.13, 1.28, 1.27, 1.26, 1.25,1.23, 1.22, 1.21 (192H, m, CH_3). $^{13}C\{^1H\}$ NMR (δ in ppm, $CHCl_3$): 174.3, 174.1, 174.0, 173.9, 173.8, 173.4, 173.0, 172.7, 172.6, 172.5, 172.4, 172.3, (C=O), (C Cp could not be identified), 62.3, 62.2, 62.0, 60.5, 60.6, 60.4 (OCH_2) 53.4, 53.3, 53.0, 51.7, 51.6, 51.5, 51.4 (CH^{α}−Glu), 33.2, 32.0, 31.9, 30.7, 30.2, 30.0, 27.4, 27.3, 27.2, 27.0, 26.8, 26.5, 26.4 (CH_2−Glu), 14.2, 14.1,14.0 (CH_3).

NMR Studies. All NMR self-diffusion experiments were carried out using a Bruker Avance 500 MHz spectrometer equipped with a 5 mm TXI probe. Only the z-axis gradients were employed in the self-diffusion studies. The pulse sequence ledbpgp2s was used with the DOSY software incorporated in the Bruker XWINNMR 3.5 p6 software suite.[33] A one-dimensional variant of the above pulse sequence was used to calibrate the diffusion delays used in the two-dimensional experiment. The ledbpgp2s pulse program is designed to minimize the effects of longitudinal eddy currents that are a consequence of the pulse field gradients required for the experiment.

Each 1D spectrum in the pseudo-2D DOSY experiment was acquired with 32 scans and 16 dummy scans. 32 slices were recorded in each 2D DOSY experiment where the z gradient was varied in equal steps from 2% to 95% of its maximum. The maximum attenuation of the signal was calibrated in a 1D version of the experiment so that all resonances were still distinguishable from the noise. The delay δ had values from 50 to 100 ms while the value for Δ ranged from 1.4 to 2.6 ms. All experiments were carried out at 300 K.

Scheme 1. Synthetic Route for the Synthesis of Generation 1 (G1) (i) HOBt/EDC/ Et_3N/CH_2Cl_2

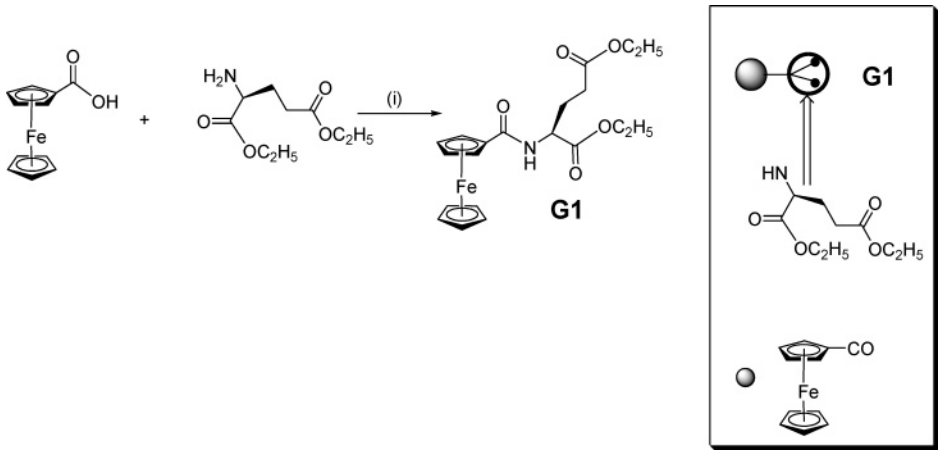

The intensity of the proton resonance is described by the Stejskal−Tanner equation from which the self-diffusion coefficient (D) is derived.

$$I = I_0 e^{-D(4\pi^2\gamma^2 g^2 \delta^2)(\Delta - \delta/3)}$$

where γ is the magnetogyric ratio for the proton, δ and Δ are the two delays within the pulse sequence when self-diffusion might occur, and g is the gradient strength at the that instant.[34−36] The most intense methyl peak (δ 1.2−1.4) was used for the determination of the self-diffusion coefficient. The particular peak necessarily changed as the generation number increased. Two clearly defined methyl resonances were visible for the **G1** and **G2** systems while in **G5** and **G6** they were highly overlapped in the region.

Electrochemical Studies. All electrochemical experiments were carried out at room temperature (296 ± 1 K) on a CV-50W voltammetric analyzer (BAS) using a conversional three-electrode cell system of glassy carbon (BAS 3.0 mm diameter) as working electrode, Pt wire as counter electrode, and Ag/AgCl (3.0 M NaCl, BAS) as a reference electrode. 0.2 M TBAP was used as the supporting electrolyte for all experiments in $CHCl_3$. Except where stated, the scan rate for CV was 100 and 25 mV s^{-1} for DPV. iR compensation was applied to all voltammetric measurements. For the cyclic voltammetric (CV) studies, the carbon electrodes were cleaned by polishing on microcloth pads with aluminum slurry. The polished electrodes were then rinsed with copious amounts of Millipore water followed by the experimental solvent. To ensure reproducibility, the working electrode was cleaned between runs. For the determination of the diffusion coefficients, experiments were run at 50, 100, 200, 300, and 400 mV s^{-1}. Determination of the heterogeneous electron-transfer rates k was calculated from simulations of the experimental data on a CHI 660B electrochemical workstation.

Results and Discussion

Synthesis and Characterization. The syntheses of ferrocene glutamic acid ester dendrimers (**G1**−**G6**) are summarized in Schemes 1 and 2. While as a direct combination of Fc−COOH and N−GluOEt·HCl gave the first generation **G1** (Scheme 1), a convergent strategy[31,32] was adopted for the synthesis of the larger dendrimers via the Boc-protected peptide dendrimers derivatives (**Boc-G2** to **Boc-G6**), followed by coupling to Fc-COOH to generate **G2**−**G6** (Scheme 2). Despite the potential steric inhibition of the amino group in **Boc-G6**, the reaction with Fc-COOH results in the formation of **G6** in relatively high yields. We speculate that this is due to the enhanced solubility of **Boc-G6** in dichloromethane, which may be allow better penetration into the center of dendrimer and enable a more facile reaction with the Fc synthon.

The dendrimers **G1**−**G6** were obtained as orange solids after purification by column chromatography. The purity of these dendritic compounds was also confirmed by reverse phase HPLC analysis. Figure 1 shows HPLC traces of **G1**−**G6** eluted as single peaks with increasing elution time with increase in dendrimer size for **G1**−**G4**. Interestingly, **G5** and **G6** eluted earlier than some of the lower generations, suggesting a change in the hydrophobicity for the higher dendrimer generations, most likely due to a change in the dendrimer surface, as a result of dendron backfolding and globulization.

All compounds were investigated spectroscopically by ^{1}H (1-D, 2-D COSY, HMQC and TOCSY) and $^{13}C\{^1H\}$-NMR, UV−vis, and mass spectrometry (ESI-MS) (see Supporting Information Figure S1 ^{1}NMR spectra of all generations). The algebraic increase in the number of NH's (^{1}H NMR) and C=O (^{13}C NMR) with increasing generation demonstrates the successful syntheses of dendrimers **G1**−**G6**. For example, the ^{1}H NMR for **G1**−**G4** exhibits 1, 3, 7, and 15 amide NHs, respectively. The $^{13}C\{^1H\}$ NMR for **G1** shows three signals for the three amide C=O, while 17 of the possible 31 C=O resonances are observed for **G4**. In **G5** and **G6** the amide and carbonyl peaks are overlapping, preventing the assignment of the individual signals.

The protons of the Fc group in compounds **G1**−**G4** exhibit signals characteristic of monosubstituted ferrocene derivatives with the ortho-H exhibiting signals in the range of δ 4.90−4.60, downfield from the meta-Hs (δ 4.40−4.20), and a singlet for the unsubstituted Cp ring in the range of δ 4.20−4.10.[16,38,39] In **G1**, two resonances are observed for the two magnetically nonequivalent o-H (δ 4.66 and δ 4.75) while for **G3** and **G4** single peaks are observed at δ 4.60 and δ 4.58, respectively. In **G5** the o-, m-, and the H atoms on the unsubstituted Cp are all shielded and occur at δ 4.16, 4.20, and 4.30, respectively. In general, the signals of the Fc group are experiencing an increased shielding on going from **G1** to **G6**, indicating the gradual modification of the environment about the Fc group as a consequence of its encapsulation by the dendritic peptide.

Despite the repetitive nature of the sequence, the amide NH signals for **G1**−**G6** are spread over a remarkably large range of chemical shifts (δ 6.0−9.0), suggesting different environments of the amide protons. The signals for **G1**−**G4** are well-resolved whereas for

Scheme 2. Schematic View of the Synthesis of Fc−Peptide Dendrimers G2−G6: (a) HOBt/EDC/Et_3N/CH_2Cl_2, (b) TFA/CH_2Cl_2 Followed by (c) FcCOOH/HOBt/EDC/Et_3N/CH_2Cl_2

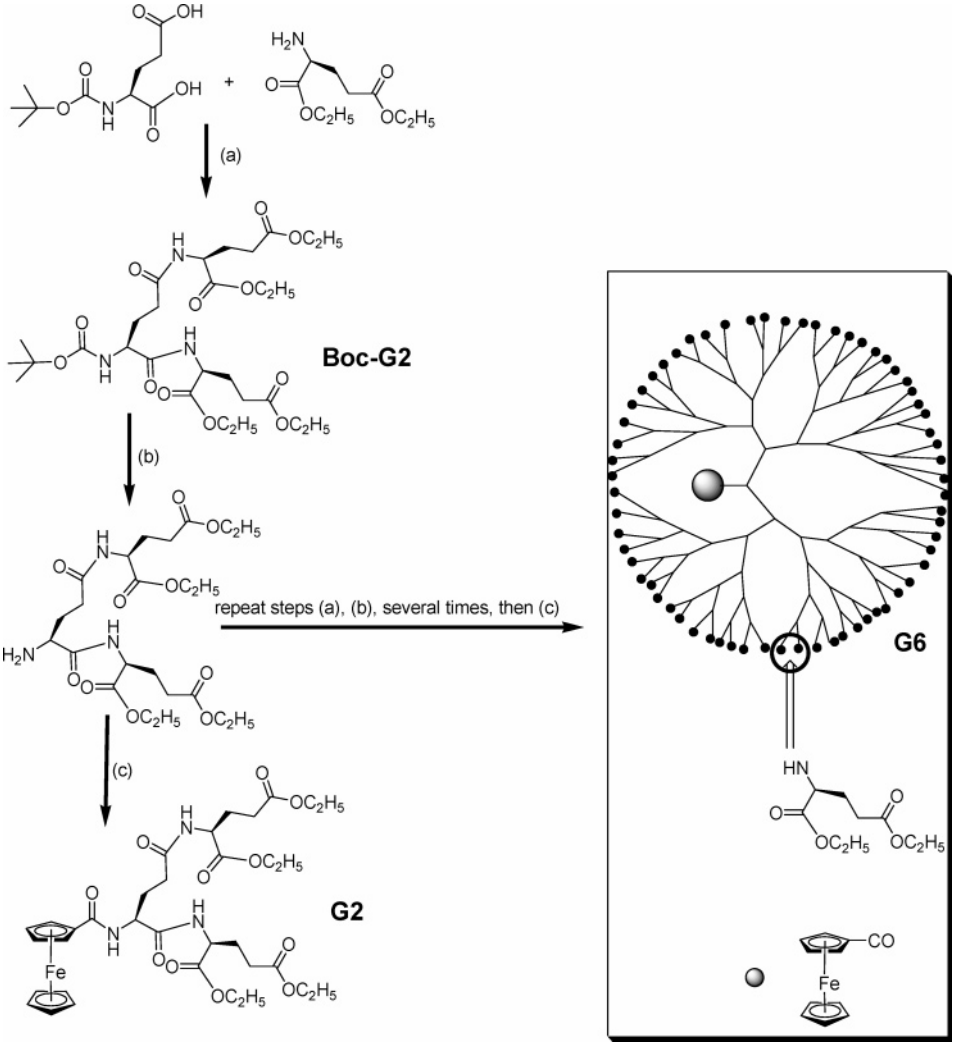

G5 and **G6** the amide peaks overlap. A wide range of amide NH shifts were also reported for other peptide and polyamide dendrimers.[29,40,41] In general, deshielding of the amide protons beyond δ 7.5 is rationalized by the involvement of the amide NH in H-bonding.[40,42,43] In poly(glutamic acid) dendrimers having adamantine cores, the amide NH resonance shifts to lower field with each successive generation.[28] The CH− stretching vibration of the ferrocene moiety in the solid state decreases consistently from 3102 cm^{-1} in **G1** to 3071 cm^{-1} in **G6** (see Table S1 of the Supporting Information), which further indicate the gradual attenuation of the Fc core by the dendritic shield.

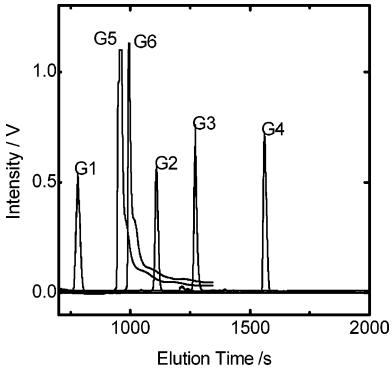

Figure 1. HPLC traces of dendrimers **G1**−**G6** using a reverse phase column C18 and CH_3CN/H_2O (1%TFA) (98:2) as the eluent.

CD spectra of 2 mM concentrations of **G1**=**G6** were recorded in MeOH and are shown in Figure 2. The band

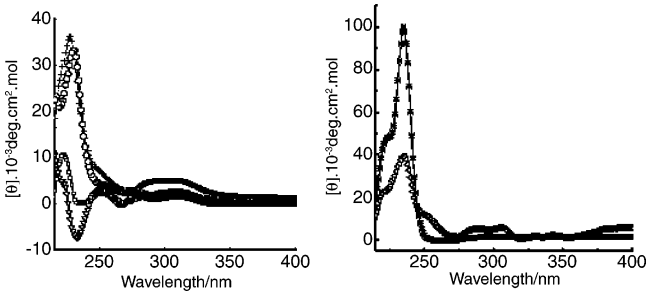

Figure 2. CD spectra of 2 mM concentrations of (left) **G1** (△), **G2** (□), **G3** (- - -), **G4** (+), (right) **G5** (○), and **G6** (●) recorded in MeOH.

associated with the n−π^* of CONH in these dendritic peptides is observed at 230 nm for **G1** and **G2** having a negative Cotton effects, whereas for **G3**−**G6** a positive Cotton effect is observed at 225 nm.[44−47] The maximum mean residue molar ellipticities value for this transition, as calculated from eq 1, increase from 10 for **G1** to 100 for **G6**. In addition, a band with a negative Cotton is observed at 260 nm in **G1**−**G3** but is absent in higher

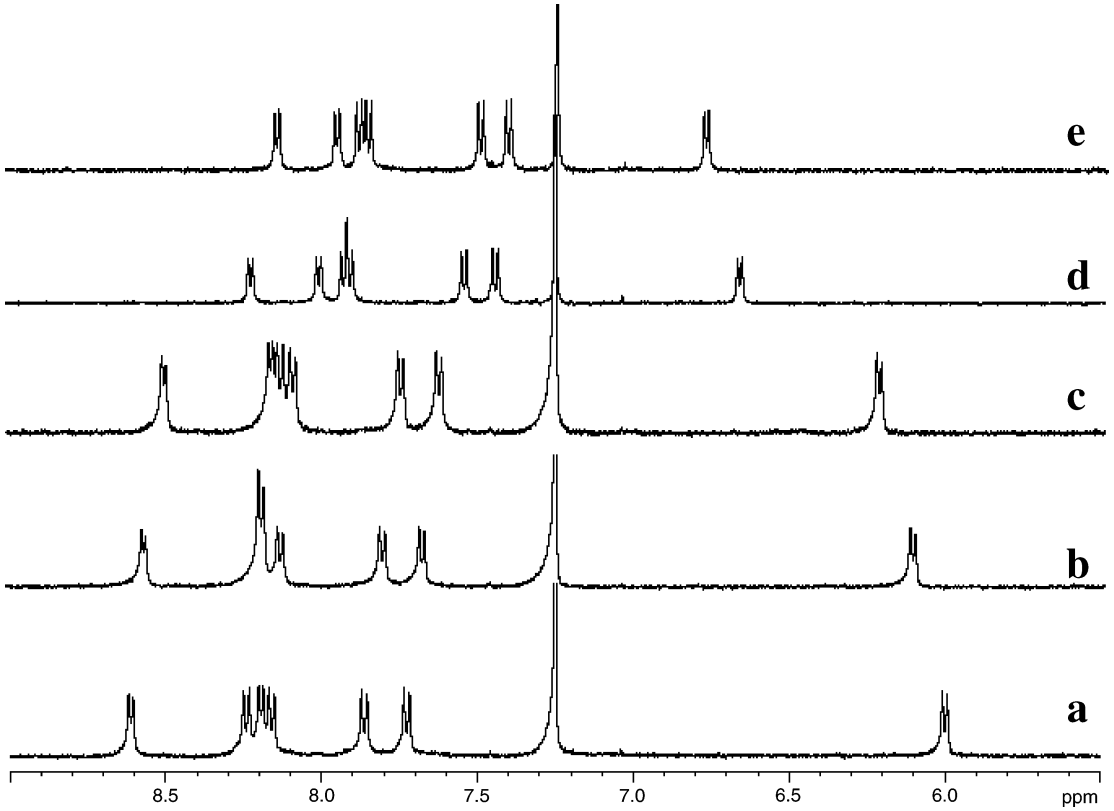

Figure 3. Effect of DMSO-d_6 addition to the amide NH. Partial ^{1}H NMR spectrum of **G3** in $CDCl_3$ with addition of DMSO-d_6 (a) 0%, (b) 5%, (c) 10%, (d) 15%, and (e) 20% DMSO-d_6 added.

Table 1. Amide Stretching Vibrations, Absorbances, and Absorbance Ratios for H-Bonded and Non-H-Bonded N−H for Dendrimers G1−G6

	freq (cm^{-1})/ A_{Non-HB}	freq (cm^{-1})/ A_{H-B}	absorbance ratios A_{H-B}/A_{Non-HB}
G1	3432/0.018	3377/0.006	0.3
G2	3425/0.0.33	3335/0.075	2.3
G3	3425/0.034	3329/0.158	4.6
G4	3422/0.156	3330/0.338	2.1
G5	3422/0.102	3325/0.652	6.4
G6	3422/0.114	3327/0.817	7.1

generation **G4**−**G6** and is associated with the Fc-amide.[46,47]

Evaluation of Hydrogen Bonding. The association of the amide groups in dendrimers **G1**−**G6** via hydrogen bonding was investigated by means of FT-IR and ^{1}H NMR spectroscopies of chloroform solutions. Table 1 shows the data derived from N−H stretching region of the FTIR spectrum for **G1**−**G6**. In all cases, two signals are observed at 3320−3440 cm^{-1}: the one to higher energy being due to non-H-bonded amide NH and the one at lower energy being due to H-bonded amide NH.[42,48,49] Our data suggest that the amount of associated amide groups and the strength of hydrogen bonding increased with rising generations. Even at low concentration, intramolecular hydrogen bonding is present in these systems (Figure S4). The ratio of H-bonded to non-H-bonded amide NH (A_{H-B}:$A_{non-H-B}$) relates to the proportion of molecules engaged in intramolecular H-bonding for a given system and is summarized in Table 1. When A_{H-B}:$A_{non-H-B} \approx 1$, an equilibrium distribution exists between the free and H-bonded NH. A value larger than unity indicates a favorable H-bonded system, whereas a value smaller than unity suggests a predominately non-H-bonded system.[50−52] Our studies show that this ratio increases from 0.3 in **G1** to 7.0 in **G6**. We also noted a discontinuity in this trend at **G4**. The amide NH stretching vibration was observed to decrease from 3377 cm^{-1} in **G1** to 3327 cm^{-1} in **G6**, lending support to our interpretation of an increased intramolecular H-bonding with increase in generation.[53]

Studies by Ranganthan and Kurur[28] on polyglutamate dendrimers suggest that upon dendrimer growth the shape changes from an open W-shaped architecture to a compact spheroid shapes. Phenylalanine-terminated dendrimers display a significant folding back of the dendrites in the higher generations.[54] In our systems, we can expect a similar behavior with respect to encapsulation at higher generations. Furthermore, we observe that the H-bonding increases for higher generations.

To further investigate the H-bonding in the dendrimers, we carried out variable temperature (VT) NMR of the dendrimers and DMSO addition experiments. The amide chemical shifts (δ_{NH}) in a nonpolar solvent, such as $CDCl_3$, are sensitive to the amide group's involvement in H-bonding. The temperature dependence of amide NH provides an indication of the efficacy of H-bonding but is by no means an absolute measure of its strength. Temperature coefficients of less than −4 ppb K^{-1} generally suggest either non-H-bonded NHs or NHs locked in a very strongly H-bond bond.[43,55] Table S2 summarizes the experimentally observed temperature coefficents for **G1**−**G4**. We make two observations: (a) the temperature coefficients are significantly greater than the threshold limit, indicating significant H-bonding; (b) the temperature coefficients are similar at both low and high concentrations, suggesting that intramolecular H-bonding is present in these dendrimers. Interestingly, the amide NH proximal to the Fc core in **G4** does not exhibit any significant temperature dependence, suggesting that it maybe locked in a strong

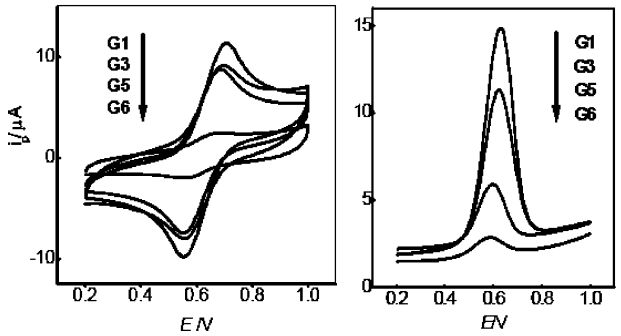

Figure 4. CV (a) and DPV (b) of **G1**, **G3**, **G5**, and **G6** ($c_{\text{dendrimer}}$ = 0.5 mM; glassy carbon working electrode, Pt counter electrode, Ag/AgCl reference electrode, 0.2 M TBAP supporting electrolyte, scan rate = 100 mV s^{-1} for CV and 25 mV s^{-1} for DPV at 23 ± 1 C).

Table 2. Electrochemical Data of 0.5 mM Dendrimers at Glassy Carbon Working Electrode, Ag/AgCl Reference Electrode, 0.2 M TBAP Supporting Electrolyte 100 mV s^{-1} at 23 ± 1 °C and UV/Visible Data for Dendrimers in $CHCl_3$

	G1	G2	G3	G4	G5	G6
$E_{1/2}$/ mV[a]	633 (5)	630 (5)	627 (4)	625 (5)	620 (3)	607 (6)
ΔE_p/mV[a]	130 (9)	115 (5)	124 (7)	113 (5)	120 (5)	115 (6)
$E_{1/2}$(DPV)/mV[b]	642 (6)	636 (5)	635 (6)	624 (9)	608 (5)	603 (3)
ΔE_p/mV[b]	20 (3)	28 (2)	24 (4)	40 (5)	24 (2)	28 (3)
i_c/i_a [a]	1.0	1.1	1.1	1.1	1.0	1.0
λ_{max}/nm	442	440	444	446	432	427
ϵ/M^{-1} cm^{-1}	422	413	394	292	151	64

[a] CV. [b] DPV, standard deviation in parentheses, $E_{1/2} = (E_O + E_R)/2$, $\Delta E_P = |E_O - E_R|$.

intramolecular H-bond (Figures S2 and S3, Table S2).[43,54,55] Because of the strong overlap of the amide NH in **G5** and **G6**, it was impossible to assign individual signals to specific groups.

Addition of a H-bond-accepting solvent such as DMSO to $CDCl_3$ solutions of the dendrimers **G1**−**G4** allows for identification of intramolecular hydrogen-bonded NH groups.[56−58] Addition of small amounts of d_6-DMSO brought about monotonic downfield shifts of the exposed NH groups (NH1) in peptides an example is presented for **G3** (Figure 3). Whereas the "unexposed" NH groups are slightly shifted upfield or relatively uneffected, the exposed amide NHs experience a downfield shift, consistent with the formation of H-bonds between the exposed NH groups and DMSO.[56−58] This observation fits into the picture of surface amides being involved in intermolecular interactions via H-bonding.

Effects of Ferrocene Encapsulation on the Redox Properties. The effect of the dendritic sphere on the redox properties of dendrimers **G1**−**G6** was investigated by electrochemical methods. A representative cyclic voltammetry (CV) and differential pulse voltammogram (DPV) of some of the dendrimers is shown in Figure 4. The CVs for all systems showed quasi-reversible one-electron oxidation waves with peak potential separations of 115−130 mV (CV), and ratio of the peak current i_p is close to unity. Importantly, the $E_{1/2}$ (CV) shows a dependence on the dendritic generation and is shifted from $E_{1/2}$ = 633(5) mV for **G1** to 607-(6) mV for **G6**. Small decreases in $E_{1/2}$ for Fc-core dendrimers were reported before, reflecting the stabilization of the oxidized Fc core by the dendritic environment.[9] Thus, the cathodic shift is consistent with a more compact hydrophobic dendritic environment at higher generations.[59,60] In addition, the peak current is drastically reduced as goes from **G1** to **G6**.

It maybe expected that a completely shielded Fc core does not display any redox activity.[61] However, one has to bear in mind the redox properties of the peptide dendrimers described here are governed by the inherent charge-transfer properties of the peptide itself. From modeling of the CVs (Digisim software, Bioanalytical Systems), we were able obtain the heterogeneous electron-transfer rate constant k^0. As expected for a redox active core that experiences increasing encapsulation with each successive dendrimer generation,[6,9,62,63] k^0 decreases for **G1** to **G6** (see Table 3).

The diffusion coefficients were obtained using cyclic voltammetry and by the PGSE NMR method and are listed in Table 3. The CV measurements on **G1**−**G6** allow us to obtain the diffusion coefficients using the Randles−Sevcik equation (Supporting Information S3). These diffusion coefficients correspond to the diffusive properties of the dendrimers in an electric field. In addition, we determined the diffusion coefficients by NMR methods, using the Stejskal−Tanner equation. These measurements allow us to evaluate the diffusive properties of the uncharged dendrimers in solution. Again, we find that an increase in the dendrimer generation results in a decrease of the diffusion coefficient. It is noteworthy to point out the large difference in the D_0(CV) for **G5** and **G6**. In contrast, the D_0(NMR) values are very similar, suggesting a significantly different diffusive behavior of the two dendrimers under an applied potential.

Using the Stokes−Einstein relationship (eq 2), we were able to determine the hydrodynamic radius r_H for all dendrimers. As expected, with increasing dendrimer generation, the effective size of the dendrimer measured by r_H increases.

$$D_0 = \frac{kT}{6\pi\eta r_H} Z \qquad (2)$$

This is also supported by molecular modeling using Spartan (Figure 5), which allows us to visualize the encapsulation of the Fc core and provides the diameter

Table 3. Physical Dimensions of Dendrimers

	G1	G2	G3	G4	G5	G6
no. of terminal groups	2	4	8	16	32	64
mol wt	415	730	1358	2615	4616	7659
$D_o \times 10^6$/cm^2 s^{-1} (CV)	8.1 (1.8)	6.7 (1.0)	5.2 (0.8)	4.7 (0.8)	4.2 (0.7)	0.8 (0.1)
$D_o \times 10^5$/cm^2 s^{-1} (NMR)	6.4 (0.1)	7.0 (0.1)	1.73 (0.02)	0.90 (0.04)	0.355 (0.002)	0.384 (0.003)
$k \times 10^3$/cm s^{-1}	20.2 (3.0)	10.4 (2.0)	8.2 (1.0)	7.0 (2.0)	6.5 (1.0)	0.6 (0.1)
r_H/Å (CV)	6.0	7.3	9.4	10.4	13.6	60.8
r_H/Å (NMR)	0.8	0.7	2.9	5.7	14.3	13.3
diameter[a]/Å	9	14	17	21	27	34

[a] From Spartan modeling, standard deviation in parentheses, D_0(CV) = diffusion coefficient obtained by cyclic voltammetry, D_0(NMR) − D_0 obtained by PGSE NMR.

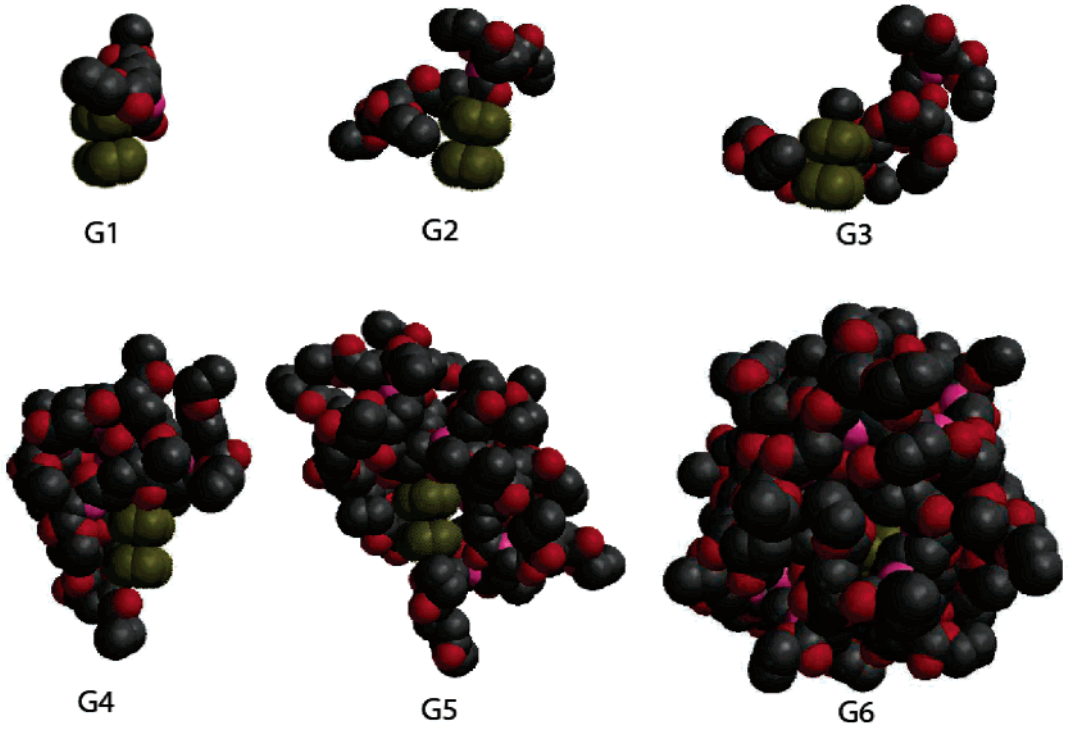

Figure 5. Spatan models of compounds **G1**−**G6** (red oxygen, violet nitrogen, black carbons), showing the presence of the Fc moiety (olive) and the encapsulation of the Fc core in **G6**. H atoms are omitted for clarity.

of the bare dendrimer lacking the solvation shell, which increases with dendrimer generation.

Our own attempt at molecular modeling (Figure 5) shows complete encapsulation of the Fc core for **G6**. However, the solution electrochemistry indicates that even at **G6** the dendrimers exhibit communication between the Fc core and the working electrode, which may indicate an incomplete encapsulation once in contact with the electrode or potentially signifies the inherent charge-transfer ability of the dendritic peptide.

In conclusion, we report the synthesis of the first peptide dendrimers having a ferrocene core. These dendrimers show an attenuation of the redox properties of the Fc group indicating the encapsulation of the central core at generation 6 (**G6**). These systems appear as well-defined structural entities, stabilized by strong intramolecular H-bonding in particular in higher generations. The dendritic enviroment may offer a strong and specific affinity for guest molecules, potentially making these systems useful receptors for small molecules for the transport and delivery of drugs. In principle, this process can be monitored electrochemically. We are currently exploring the effect of ester deprotection, which should also offer multiple binding sites for metal ions and cationic molecules.

Acknowledgment. The authors acknowledge the financial support from NSERC, the Canada Foundation for Innovation and the Saskatchewan Innovation Fund. F.E.A. is recipient of a Commonwealth scholarship. H.-B.K. is the Canada Research Chair in Biomaterials. We are grateful to Ken Thoms for the MS and the SSSC for the NMR instrument time, S. Chowdhury for assistance with 2D NMR, and Dr. Subrata Dey for assistance with HPLC analysis.

Supporting Information Available: NMR spectra of dendrimers, FT-IR spectra of the amide A region of all dendrimers, CV at various scan rates for determining D_0, and tables of spectroscopic analysis. This material is available free of charge via the Internet at http://pubs.acs.org.

References and Notes

(1) Burroughes, J. H.; Bradley, D. D. C.; Brown, A. R.; Marks, R. N.; McKay, K.; Friend, R. H.; Burn, P. L.; Holmes, A. B. *Nature (London)* **1990**, *347*, 539.
(2) Zhu, Z.; Moore, J. S. *J. Org. Chem.* **2000**, *65*, 116−123.
(3) Halim, M.; Pillow, J. N.; Samuel, I. D. W.; Burn, P. L. *Adv. Funct. Mater.* **1999**, *11*, 371−374.
(4) Pillow, J. N.; Halim, M.; Lupton, J. M.; Burn, P. L.; Samuel, I. D. W. *Macromolecules* **1999**, *32*, 5985−5993.
(5) Cameron, C. S.; Gorman, C. B. *Adv. Funct. Mater.* **2002**, *12*, 17−20.
(6) Cardona, C. M.; Mendoza, S.; Kaifer, A. E. *Chem. Soc. Rev.* **2000**, *29*, 37−42.
(7) Cardona, C. M.; McCarley, T. D.; Kaifer, A. E. *J. Org. Chem.* **2000**, *65*, 1857−1864.
(8) Dandliker, P. J.; Diederich, F.; Gisselbrecht, J.-P.; Louati, A.; M.; G. *Angew. Chem., Int. Ed. Engl.* **1995**, *34*, 2725−2728.
(9) Cardona, C. M.; Kaifer, A. E. *J. Am. Chem. Soc.* **1998**, *120*, 4023−4024.
(10) Wang, Y.; Cardona, C. M.; Kaifer, A. E. *J. Am. Chem. Soc.* **1999**, *121*, 9756−9757.
(11) Stone, D. L.; Smith, D. K.; McGrail, P. T. *J. Am. Chem. Soc.* **2002**, *124*, 856−864.
(12) Chowdhury, S.; Schatte, G.; Kraatz, H.-B. *J. Chem. Soc., Dalton Trans.* **2004**, *11*, 1726−1730.
(13) Baker, W. S.; Lemon, B. I. I.; Cooks, R. M. *J. Phys. Chem. B* **2001**, *105*, 8885−8894.
(14) Kraatz, H.-B.; Galka, M. *Met. Ions Biol. Syst.* **2001**, *38*, 385−409.
(15) Galka, M.; Kraatz, H.-B. *ChemPhysChem* **2002**, *3*, 356−359.
(16) Kraatz, H.-B.; Leek, D. M.; Houman, A.; Enright, G. D. *J. Organomet. Chem.* **1999**, *589*, 39.
(17) Xu, Y.; Kraatz, H.-B. *Tetrahedron Lett.* **2001**, *42*, 2601−2603.
(18) Xu, Y.; Saweczko, P.; Kraatz, H.-B. *J. Orgamet. Chem.* **2001**, *637*−*639*, 335−342.
(19) Xu, H.; Kinsel, G. R.; Zhang, J.; Li, M.; Rudkevich, D. M. *Tetrahedron* **2003**, *59*, 5837−5848.
(20) Chow, H.-F.; Mong, T. K.-K.; Chan, Y.-H.; Cheng, C. H. K. *Tetrahedron* **2003**, *59*, 3815−3820.
(21) Kim, Y.; Zeng, F.; Zimmerman, S. C. *Eur. J. Chem.* **1999**, *5*, 2133.

(22) Newkome, G. R.; Moorefield, C. N.; Epperson, J. D. *Eur. J. Org. Chem.* **2003**, 3666−3672.
(23) Newkome, G. R.; Lin, X.; Weiss, C. D. *Tetrahedron: Asymmetry* **1991**, *2*, 957.
(24) Dykes, G. M.; Brierley, L. J.; Smith, D. K.; McGrail, T. P. *Eur. J. Chem.* **2001**, *7*, 4730−4739.
(25) Brouwer, A. J.; Mulders, S. J. E.; Liskamp, R. M. J. *Eur. J. Org. Chem.* **2001**, 1903−1915.
(26) Twyman, L. J.; Beezer, A. E.; Mitchell, J. C. *Tetrahedron Lett.* **1994**, *35*, 4423.
(27) Twyman, L. J.; Beezer, A. E.; Esford, R.; Mathews, B. T.; Mitchell, J. C. *J. Chem. Res. Synop.* **1998**, *12*, 758−759, 3408−3415, 3417−3460.
(28) Ranaganathan, D.; Kurur, S.; Gilardi, R.; Karle, I. L. *Biopolymers* **2000**, *54*, 289−295.
(29) Ranaganathan, D.; Kurur, S. *Tetrahedron Lett.* **1997**, *38*, 1265−1268.
(30) Ranaganathan, D.; Kurur, S.; Madhusudanan, K. P.; Roy, R.; Karle, I. *J. Pept. Res.* **1998**, *51*, 297.
(31) Vinogradov, S. A.; Lo, L.-W.; Wilson, D. F. *Eur. J. Chem.* **1999**, *5*, 1338−1347.
(32) Vinogradov, S. A.; Wilson, D. F. *Eur. J. Chem.* **2000**, *6*, 2456−2461.
(33) Wu, D.; Chen, A.; Johnson, J. C. S. *J. Magn. Reson. A* **1995**, *115*, 260−264.
(34) Goldsmith, J. I.; Takada, K.; Abruna, H. D. *J. Phys. Chem. B* **2002**, *106*, 8504−8513.
(35) Ihre, H.; Hult, A.; Suderlind, E. *J. Am. Chem. Soc.* **1996**, *118*, 6388−6395.
(36) Soderman, O.; Stilbs, P. *Prog. Nucl. Magn. Reson. Spectrosc.* **1994**, *26*, 445−482.
(37) Romagnoli, B.; van Baal, I.; Price, D. W.; Harwood, L. M.; Hayes, W. *Eur. J. Chem.* **2004**, 4148−4157.
(38) Kraatz, H.-B.; Lusztyk, J.; Enright, G. D. *Inorg. Chem.* **1997**, *36*, 2400.
(39) Ashton, P. R.; Balzani, V.; Clemente-Leon, M.; Colonna, B.; Stoddart, J. F.; Credi, A.; Jayaraman, N.; Raymo, F. M. *Eur. J. Chem.* **2002**, *8*, 673−684.
(40) Jiang, H.; Leger, J.-M.; Dolain, C.; Guionneau, P.; Huc, I. *Tetrahedron* **2003**, *59*, 8365−8374.
(41) Boas, U.; Karlsson, A. J.; de Waal, B. F. M.; Meijer, E. W. *J. Org. Chem.* **2001**, *66*, 2136−2145.
(42) Gung, B. W.; Zhu, Z. *Tetrahedron* **1996**, *37*, 2189−2192.
(43) van Staveren, D. R.; Weyhermuller, T.; Metzler-Nolte, N. *Dalton Trans.* **2003**, 210−220.
(44) Muraoka, T.; Kinbara, K.; Kobayashi, Y.; Aida, T. *J. Am. Chem. Soc.* **2003**, *125*, 5612−5613.
(45) Takeuchi, M.; Mizuno, T.; Shinkai, S.; Shirakami, S.; Iroh, T. *Tetrahedron: Asymmetry* **2000**, *11*, 3311−3322.
(46) Love, C. S.; Hirst, A. R.; Chechik, V.; Smith, D. K.; Ashworth, I.; Brennan, C. *Langmuir* **2004**, *20*, 6580−6585.
(47) Romagnoli, B.; van Baal, I.; Price, D. W.; Harwood, L. M.; Hayes, W. *Eur. J. Org. Chem.* **2004**, 4148−4157.
(48) Gung, B. W.; Zhu, Z. *J. Org. Chem.* **1997**, *62*, 6100−6101.
(49) Gellman, S. H.; Dado, G. P.; Liang, G.; Adams, B. R. *J. Am. Chem. Soc.* **1993**, *113*, 1164.
(50) Lopez de la Paz, M.; Ellis, G.; Perez, M.; Perkins, J.; Jimenez-Barbero, J.; Vicent, C. *Eur. J. Chem.* **2002**, 840−855.
(51) Kuhn, L. P.; Schleyer, P. V. R.; Baitinger, J. W.; Eberson, L. *J. Am. Chem. Soc.* **1964**, *86*, 650.
(52) Brimacombe, J. S.; Foster, A. B.; Stacey, M.; Whiffen, D. H. *Tetrahedron* **1958**, *4*, 351.
(53) Paulini, R.; Frankamp, B. L.; Rotello, V. M. *Langmuir* **2002**, *18*, 2368−2373.
(54) Cavallo, L.; Fraternalli, F. *Eur. J. Chem.* **1998**, *4*, 927−934.
(55) Kirsten, C.; Schrader, T. *J. Am. Chem. Soc.* **1997**, *119*, 12061−12068.
(56) Hess, A.; Metzler-Nolte, N. *Chem. Commun.* **1999**, 885−886.
(57) Maji, S. K.; Banerjee, R.; Velmurugan, D.; Razak, A.; Fun, H. K.; Banerjee, A. *J. Org. Chem.* **2002**, *67*, 633−639.
(58) Maji, S. K.; Haldar, D.; Bhattacharyya, D.; Banerjee, A. *J. Mol. Struct.* **2003**, *646*, 111−123.
(59) Chasse, T. L.; Yohannan, J. C.; Kim, N.; Li, Q.; Li, Z.; Gorman, C. B. *Tetrahedron* **2003**, *59*, 3853−3861.
(60) Chasse, T. L.; Sachdeva, R.; Li, Z.; Petrie, R. J.; Gorman, C. B. *J. Am. Chem. Soc.* **2003**, *125*, 8250−8254.
(61) Turin, C.-O.; Chiffre, J.; de Montauzon, D.; Daran, J.-C.; Caminade, A.-M.; Manoury, E.; Balavoine, G.; Majoral, J.-P. *Macromolecules* **2000**, *33*, 7328.
(62) Chi, C.; Wu, J.; Wang, X.; Zhao, X.; Li, J.; Wang, F. *Macromolecules* **2001**, *34*, 3812−3814.
(63) Ong, W.; Kaifer, A. E. *J. Am. Chem. Soc.* **2002**, *124*, 9358−9359.
(64) Jayakumar, N. K.; Bharathi, P.; Thayumanavan, S. *Org. Lett.* **2004**, *6*, 2547−2550.
(65) Jayakumar, N. K.; Thayumanavan, S. *Tetrahedron* **2005**, *61*, 603−608.

MA050531D